European Review for Medical and Pharmacological Sciences 2019; 23: 7314-7326

MiR-9-5p could promote angiogenesis and radiosensitivity in cervical cancer by targeting SOCS5

Y.-Q. WEI[1,2], X.-L. JIAO[1], S.-Y. ZHANG[1], Y. XU[1], S. LI[2], B.-H. KONG[1]

[1]Department of Obstetrics and Gynecology, Qilu Hospital, Shandong University, Ji'nan, China
[2]Department of Obstetrics and Gynecology, Jinan Central Hospital, Ji'nan, China

Abstract. – OBJECTIVE: The aim of this study was to investigate the molecular mechanism of miRNA-9-5p in cervical cancer.

PATIENTS AND METHODS: The expression level of microRNA-9-5p (miR-9-5p) in cervical cancer (CC) tissues and cell lines was examined by quantitative Real Time-Polymerase Chain Reaction. Cells were transfected with Lipofectamine 3000. Cell proliferation was measured by Cell Counting Kit-8 (CCK-8). Invasion assays were performed in 24-well transwell chambers system with 8 μm pores. Cell invasion was evaluated by transwell assay. Western blot was used to detect the changes of epithelial-mesenchymal transition (EMT) and SOCS5. The effects of miR-9-5p on tubule formation were examined under different doses of γ radiation. Immunohistochemistry assay was used to analyze the protein expression of SOCS5. Fluorescence microscopy analysis was used to measure autophagosomes after cells treated with γ irradiation.

RESULTS: From the Cancer Genome Atlas (TCGA) database, the expression of miR-9-5p was significantly higher in cervical cancer patients than in the negative ones, and it was verified in 22 paired of lymph node-positive patient tissues and negative. The overexpression of miR-9-5p promoted proliferation and invasion of cervical cancer cells *in vitro* and primary tumor growth *in vivo*. MiR-9-5p reduced the tubule generation after the radiation dose of 4Gy. Besides, we identified SOCS5 as the target of miR-9-5p, and the overexpression of SOCS5 could inhibit miR-9-5p mimics from promoting tubule formation.

CONCLUSIONS: MiR-9-5p could promote proliferation and invasion of CC cells *in vitro* and *in vivo*. MiR-9-5p could affect angiogenesis and radiosensitivity of CC cells by targeting SOCS5.

Key Words:
MiR-9-5p, Cervical cancer, Metastasis, Radiosensitivity, SOCS5.

Introduction

Cervical Cancer (CC) is a common gynecological malignancy and a leading cause of cancer-associated mortality in female worldwide[1], especially in developing countries. Although cervical cancer screening has gained popularity around the world, there are still a large number of advanced diseases, especially in developing countries including China[2]. Radiotherapy is the most common intervention, as either a primary or adjuvant therapy. However, the 5-year survival rate for patients with advanced cervical cancer is still about 66%[3], suggesting a need to improve the radiosensitivity of cervical cancer. However, the mechanism by which cell radiosensitivity is regulated is not known in cervical cancer. It has been reported that metastasis to lymph nodes and distant organs are the main cause of treatment failure for cervical cancer[4]. Therefore, the development of effective treatments is of great significance for the aggressive expansion of the disease. It is necessary to further elucidate the molecular mechanism of lymph node metastasis.

MicroRNA (miRNA) is a group of short and non-coding RNAs which are involved in the regulation of gene expression by complementary base pairing with the 3`-UTR of mRNA and trigger translation repression or RNA degradation[5-7]. Their deletion, amplification or aberrant expression may affect tumorigenesis, including migration and invasion of cancer cells, which may make them an effective tool for diagnosis, prognosis, and treatment of cancer[8]. MiR-9 has been found to act as an oncogene or tumor suppressor in different types of cancer[9,10]. MiR-9-5p, as a mediator of hypoxic injury in cardio myoblasts, could prevent cardiac remodeling after acute myocardial infarction (MI) under suppressed[11].

Corresponding Author: Beihua Kong, MD; e-mail: kongbeihua@sdu.edu.cn

MiR-9-5p promotes mesenchymal stem cells migration by upregulating β-catenin signaling pathway[12]. Overexpression of miR-9-5p inhibited CXCR4 reducing high glucose-induced injury in HUVECs[13]. In addition, it has reported that miR-9-5p, as a specific for HPV, could induce cervical malignancies[14]. Despite these studies, the role of miR-9-5p in cervical cancer lymph node metastasis remains unclear. Therefore, understanding how miR-9-5p play a major regulatory role in cancer initiation, progression, metastasis, and radioresistance could open up significant innovative areas for therapy cervical cancer.

In our work, the function and mechanism of miR-9-5p were explored in the progression of cervical cancer. We identified miR-9-5p as a metastasis-promoting miRNA in CC. Our data showed that the ectopic expression of miR-9-5p could motivate CC cell proliferation and invasion. Also, MiR-9-5p could affect HUVEC tube formation and CC cells autophagy. In addition, miR-9-5p affected the radiosensitivity of CC cells to γ radiation. Suppressor of cytokine signaling 5 (SOCS5) was identified as a direct interact of miR-9-5p in CC and miR-9-5p overexpression increased tube formation in CC cells, and these effects were attenuated by the enforced expression of SOCS5.

Patients and Methods

Patients and Tissue Samples

A total of 44 cases of cervical cancer patients' specimens (22 positive lymph nodes and 22 negative lymph nodes), including paired cancer tissues and para-carcinoma normal tissues, were collected for the study. All tissue cases were collected from the Department of Obstetrics and Gynecology from 2016-2018. The ethical approval was obtained from the Ethics Committee of Shandong University Qilu Hospital. All patients provided a written informed consent.

Cell Culture and Reagents

Cervical cancer cell lines SiHa, human umbilical vein endothelial cells (HUVEC) were purchased from American Type Culture Collection (ATCC, Manassas, VA, USA). All the cell lines were cultured in Dulbecco's Modified Eagle's Medium (DMEM; Gibco, Rockville, MD, USA) with 10% fetal bovine serum (FBS; Gibco, Rockville, MD, USA) in a humidified atmosphere of 5% CO_2 at 37°C. All the miRNA mimics and inhibitors were purchased from GenePharma (Shanghai, China). Lentiviral transfer plasmid of SOCS5 was purchased from Hanbio (Shanghai, China). GFP-LC3 adenovirus was obtained from Hanbio (Shanghai, China).

Transfection

SiHa cells were transfected with Lipofectamine 3000 (Invitrogen, Carlsbad, CA, USA) according to the manufacturer's protocol. For stable transfection, SiHa were infected with SOCS5-LV for 24 h and the cells were selected in a medium containing puromycin for 2 days.

RNA isolation and Quantitative Real Time-Polymerase Chain Reaction (qRT-PCR)

Total RNA of samples was extracted with TRIzol reagent (Invitrogen, Carlsbad, CA, USA) according to the manufacturer`s instructions. Total RNA was reverse transcribed to complementary deoxyribose nucleic acid (cDNA) using the Mir-X miRNA First-Strand Synthesis kit (TaKaRa, Dalian, China). Real Time PCR was performed using SYBR-Green qPCR master mix (TaKaRa, Dalian, China). U6 serves as an endogenous control. The primer sequences employed were as follows: U6, forward, 5'-GCTTCGGCAGCACATATACTAAAAT-3', miR-9-5p, forward, 5'-AGCTTGCTGCACCTTAGTCT-3', and the reverse was mRQ 3'primer (TaKaRa, Dalian, China).

Western Blotting

The samples were isolated with lysis buffer and left on ice for 15 min. The lysate was centrifuged at 12000 x g for 15 min at 4°C. The proteins were detected using a bicinchoninic acid (BCA) assay kit (Beyotime, Shanghai, China, P0010). The proteins were separated by sodium dodecyl sulphate-polyacrylamide gel electrophoresis (SDS-PAGE) and electro transferred to a NC membrane (Millipore, Billerica, MA, USA). The membrane was blocked with 5% non-fat milk for 2 h at room temperature and incubated with primary antibodies overnight at 4°C. After incubation with horseradish peroxidase (HRP)-labeled secondary antibodies for 2 h, the protein bands were detected using an enhanced chemiluminescence (ECL) system (GE, Little Chalfont, Buckinghamshire, UK). The primary antibodies included: anti-β-actin (1:1000, Cell Signaling Technology, Danvers, MA, USA), anti-p-mTOR (1:1000, Cell Signaling Technology, Beverly, MA, USA), anti-E-cadherin (1:1000, Cell Signaling

Technology, Danvers, MA, USA), anti-N-cadherin (1:1000, Cell Signaling Technology, Beverly, MA, USA), anti-Vimentin (1:1000, Cell Signaling Technology, Beverly, MA, USA), anti-Snail (1:1000, Cell Signaling Technology, Beverly, MA, USA), anti-LC3 (1:1000, Cell Signaling Technology, Beverly, MA, USA), anti-p62 (1:1000, Cell Signaling Technology, Beverly, MA, USA), anti-p-ULK (1:1000, Cell Signaling Technology, Beverly, MA, USA), anti-p-ERK (1:1000, Cell Signaling Technology, Beverly, MA, USA), anti-p-VEGFR2 (1:1000, Abcam, Cambridge, MA, USA), anti-VEGFA (1:1000, Abcam, Cambridge, MA, USA), anti-SOCS5 (1:1000, Abcam, Cambridge, MA, USA).

Cell Proliferation Assay

Cell proliferation was measured by the Cell Counting Kit-8 (CCK-8; BestBio, Beijing, China). Cells (2 × 103/well) were seeded into a 96-well plate and incubated overnight in the previously described conditions. Cell proliferation was monitored at different times. CCK-8 (10 μL) were subsequently added to each well and incubated for 2 h at 37°C; a microplate reader spectrophotometer (Bio-Rad, Hercules, CA, USA) was used to measure the optical density (OD) at 450 nm.

Cell Invasion Assays

Invasion assays were performed in 24-well transwell chambers system with 8μm pores. The top chamber was coated with Matrigel (BD Biosciences, Franklin Lakes, NJ, USA). The cells (5 × 104 cells in 200 μL of medium) were placed in the upper chamber and 700 μL fresh culture medium containing 15% FBS was placed in the lower chamber. After 24 h, cells penetrated through the membrane were fixed with methanol and stained with 0.05% crystal violet.

γ-irradiation

γ-irradiation experiments were performed at the Irradiation Facility of Shandong University. The medium was replaced prior to irradiation. Cells were divided into different groups and exposed under (0, 4Gy) γ-rays separately with a Siemens Primus Accelerator machine. Cells and culture medium were collected for subsequent experiments.

Tube Formation Assay

The ability of HUVEC to form network structures when treated by different conditioned media from SiHa cells was tested on Matrigel basement membrane matrix (BD Biosciences, Franklin Lakes, NJ, USA). First 60 ul Matrigel was plated per well on 96-well plates and incubated for 1 h at 37°C. HUVEC cells suspended in a different conditioned medium at a density of 3×104 /mL. After 4-6 h of incubation at 37°C, cells were examined and tube-like structures photographed using an Olympus digital camera (Olympus, Tokyo, Japan).

Immunohistochemistry

Histologically healthy and cervical cancer samples were fixed in formalin and embedded in paraffin and 4 μm thick tissue sections were cut. After blocking endogenous peroxidase, antigen retrieval, serum albumin closed the non-specific binding sites. The tissue sections were incubated at 4°C for overnight with SOCS5 (1:200, Abcam, Cambridge, MA, USA) antibodies. The next day, the slides were washed with phosphate-buffered saline (PBS) and incubated with a secondary antibody that HRP-labeled goat anti-rabbit antibodies for 30 min at room temperature. The staining was detected by treatment with diaminobenzidine (DAB; Solarbio, Beijing, China) for 1 min. Staining scores were calculated using Image-Pro Plus 6.0 (Media Cybernetics, Silver Springs, MD, USA). The final score of each sample was determined by two pathologists on the basis of intensity and extent of staining across the section.

Dual-Luciferase Reporter Assay

The 3'-untranslated regions (3'-UTR) of the SOCS5 mRNA sequence containing the putative miR-9-5p binding sites were cloned into the pmirGLO Dual-Luciferase miRNA Target Expression Vector (Promega Corporation, Madison, WI, USA). The SOCS5 mutant sequences were constructed by Genechem Co., Ltd. (Shanghai, China) and cloned into a pmirGLO vector. SiHa were co-transfected with miR-9-5p mimics and the pmirGLO vector. After 48 h, luciferase activity was measured using the Dual-Glo Luciferase Assay System.

Immunofluorescence

Autophagosomes were monitored by Nikon C-HGFI Intensilight Fiber Illuminator (Nikon, Tokyo, Japan) fluorescence microscope. Briefly, after transfected with miR-9-5p mimics, SiHa cells were then infected with GFP-LC3 adenoviral vectors (Hanbio, Shanghai, China). Fluorescence microscopy analysis was used to measure autophagosomes after cells treated with 4Gy γ irradiation.

In Vivo Studies

Animal studies were performed according to institutional guidelines. SiHa cells were stably transfected with NC or miRNA-9-5p over-expression vectors. A total of 5×106 viable cells was injected into the right flank region of nude mice (female, age, 4-5 weeks). Tumor sizes were measured using a Vernier caliper every 5 days and the tumor volume was calculated using the following formula: volume = 1/2 × length × width2. Following 4 weeks, the mice were sacrificed to determine tumor weight and volume.

Bioinformation Analyses

The TCGA miRNA expression data (http://www.tcga.org/) of cervical cancer were processed and analyzed. To identify predicted miRNA sequences that may regulate SOCS5, TargetScan (http://www.targetscan.org/) and miRanda (http://www.microrna.org/) were employed.

Statistical Analysis

Data are expressed as the mean ± standard deviation of three independent experiments. Statistical analysis was performed using Statistical Product and Service Solutions (SPSS) version 18.0 software (SPSS Inc., Chicago, IL, USA). The *t*-test was used for analyzing measurement data. Differences between the two groups were analyzed by using the Student's *t*-test. Comparison between multiple groups was done using One-way ANOVA test followed by Post-Hoc Test (Least Significant Difference). $p<0.05$ was considered a statistically significant difference.

Results

MiR-9-5p was Highly Expressed in Human CC with Positive Lymph Nodes

To verify the expression levels of miR-9-5p in lymph nodes positive and negative patients with cervical cancer, TCGA database was used to analyze the difference (Table I) and the results showed that miR-9-5p in positive lymph nodes patients was significantly higher than in negative lymph nodes patients (Figure 1A and 1B). To confirm this trend, we examined the differential expression of miR-9-5p in 22 lymph node-positive patients and 22 lymph node-negative patients. As shown in Figure 1C, the expression of miR-9-5p was significantly higher in lymph node-positive patients than in negative. The association between miR-9-5p expression and clinicopathological parameters was also analyzed that no statistically significant associations were identified (Table II). There was no significant difference in the overall survival between the two groups (Figure 1D).

MiR-9-5p Promoted Proliferation, Invasion, and Migration of Cervical Cancer Cells

We transfected SiHa with miR-9-5p mimics and inhibitor, CCK-8 assay demonstrated that interference of miR-9-5p decreased the capacity of cell proliferation in SIHA cell lines and the cell proliferation ability of the transfected miR-9-5p mimics group was higher than that of control group (Figure 2A). The effect of miR-9-5p on cell invasion and migration was evaluated by transwell assay. The results showed that compared with the control group, the invasive

Table I. The expression of miRNA in patients with positive and negative cervical cancer lymph nodes showed statistically differences from TCGA.

	logFC	Average expression	*t*	*p*-value
hsa-miR-9-3p	-0.56886	1.823811	-3.71274	0.000281
hsa-miR-191-5p	0.233048	6.010281	3.28545	0.001248
hsa-miR-9-5p	-0.65025	8.152127	-2.99976	0.003128
hsa-miR-873-5p	-0.20649	0.212552	-2.95234	0.003622
hsa-miR-378a-3p	-0.37733	6.049653	-2.78039	0.006071
hsa-miR-624-5p	-0.1973	1.021108	-2.70819	0.00749
hsa-miR-149-5p	-0.40851	4.078928	-2.6138	0.009796
hsa-miR-425-5p	0.277102	5.198176	2.597157	0.010264
hsa-miR-519a-5p	0.355264	0.439575	2.532684	0.012268
hsa-miR-375	0.834256	6.848745	2.517146	0.012801
hsa-miR-151b	0.173339	0.838116	2.498006	0.013485
hsa-miR-874-3p	0.225087	2.702216	2.48445	0.01399
hsa-miR-92b-5p	0.163392	0.454164	2.481989	0.014083
hsa-miR-3605-3p	0.12462	0.73279	2.435371	0.015959

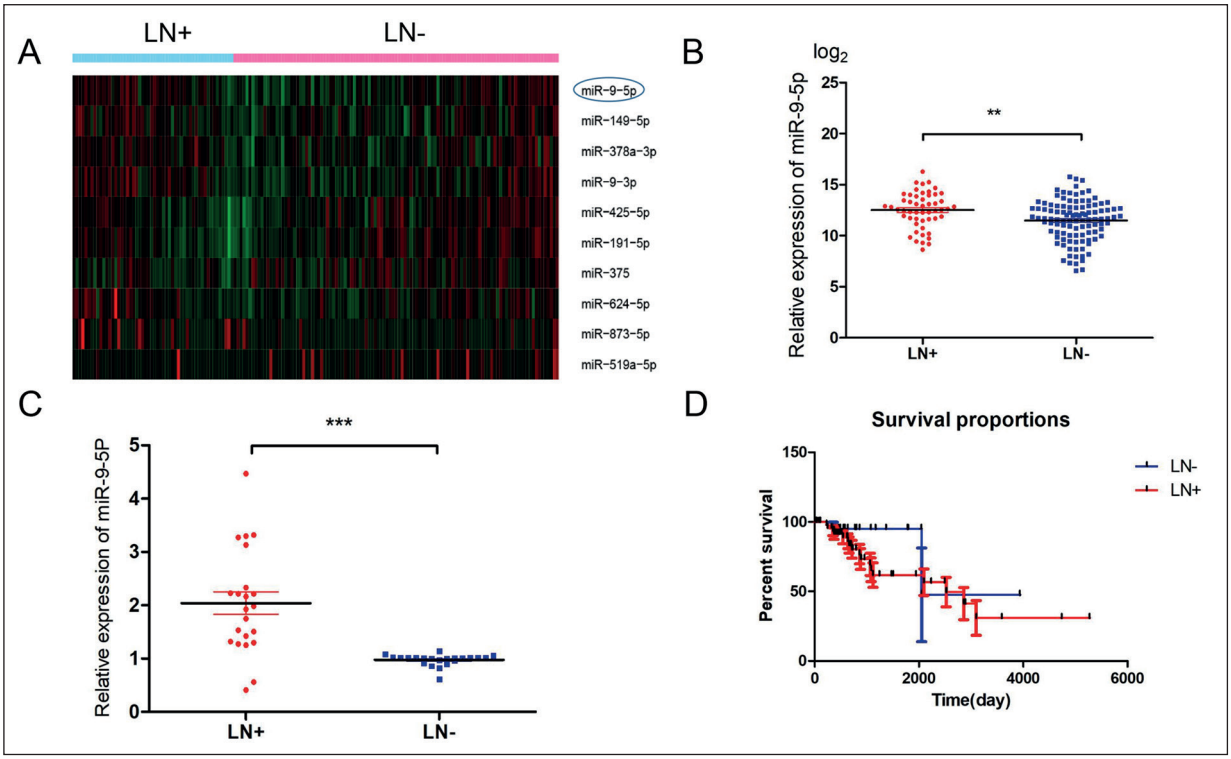

Figure 1. The high expression of miR-9-5p in positive lymph nodes of cervical cancer. ***A,*** Heat map diagram depicting expression of miRNAs dysregulated in cervical cancer from TCGA. ***B,*** The expression of miR-9-5p in positive or negative lymph nodes of cervical cancer patients from TCGA. ***C,*** Relative expression of miR-9-5p in cervical cancer patients from Qilu hospital. LN+: positive lymph nodes, LN-: negative lymph nodes. ***D,*** Overall survival of patient with CC from TCGA, divided into lymph nodes positive and negative group.

Table II. Association between miR-9-5p expression and the clinicopathological features of patients with cervical cancer.

Characteristics	Patient (n = 44)	MiR-9-5p expression		*p*
		Low (n = 23)	High (n = 21)	
Age				
< 50	35	20	15	0.202
≥ 50	9	3	6	
FIGO stage				
I	27	13	14	0.49
II	17	10	7	
Tumor diameter				
≤ 4 cm	34	19	15	0.377
> 4 cm	10	4	6	
Differentiation grade				
High	12	8	4	0.242
Middle+Low	32	15	17	
Lymph node metastasis				
Positive	22	5	17	0.000*
Negative	22	18	4	
Vasoinvasion				
Yes	28	16	12	0.392
No	16	7	9	

Note: *Denotes significant *p*-values ($p < 0.05$).

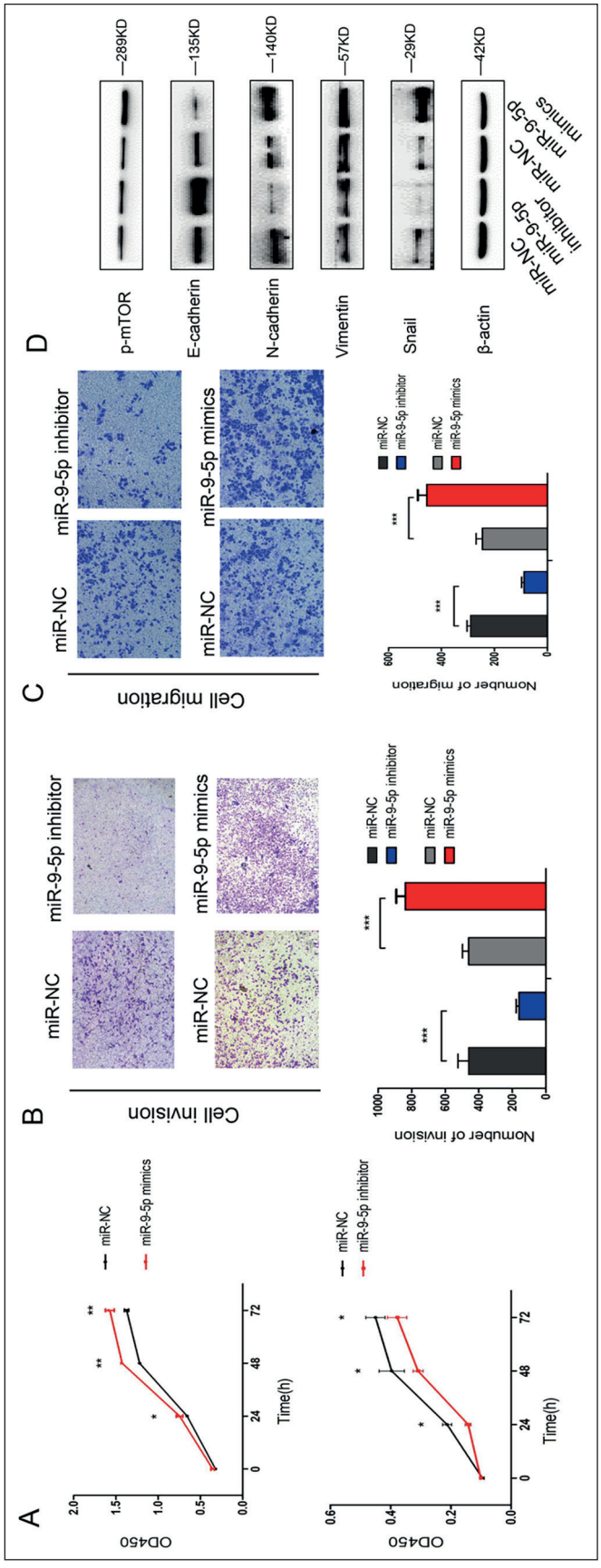

Figure 2. MiR-9-5p promoted proliferation and invasion of cervical cancer cells. ***A***, Cell viability of SiHa cells was measured by the CCK-8 assay. ***B***, MiR-9-5p effects on the invasion of SiHa cells transfected with mimics or inhibitor (magnification: 40×). ***C***, MiR-9-5p effects on the migration of SiHa cells transfected with mimics or inhibitor (magnification: 40×). ***D***, Western blot analysis of p-mTOR, E-cadherin, N-cadherin, Vimentin, Snail in miR-9-5p knockdown and overexpression compared to control group. $^{**}p<0.01$, $^{*}p<0.05$.

and migration ability of cells transfected with miR-9-5p mimics was significantly enhanced, while the invasive and migration ability of cells transfected with miR-9-5p inhibitor was decreased (Figure 2B and 2C). Western blot was used to detect the changes of epithelial-mesenchymal transition (EMT) and proliferation-related molecules after interference and overexpression of miR-9-5p. We found that knockdown miR-9-5p enhanced the expression of epithelial marker E-cadherin, while reduced mesenchymal marker N-cadherin, Vimentin, Snail and p-mTOR compared with siNC group in CC cells. On the contrary, the expression of N-cadherin, Vimentin, Snail, and p-mTOR was increased after miR-9-5p mimics transfection, while E-cadherin was downregulated (Figure 2D).

MiR-9-5p Affected the Radiosensitivity of Cervical Cancer Cells to γ Radiation

We examined the effect of miR-9-5p on tubule formation under different doses of γ radiation. The radiation dose we used was 0Gy and 4Gy, respectively. Without irradiation, tubule generation increased in miR-9-5p mimics group compared with control group (Figure 3A and 3B). After the radiation dose of 4Gy, tubule generation in miR-9-5p mimics group was significantly reduced compared with that in control group. It has been reported that radiotherapy is associated with autophagy, we speculated that miR-9-5p might affect radiation by autophagy. First, we monitored autophagosome by fluorescence microscopy in the SiHa cells infected with GFP- LC3 adenovirus. As shown in Figure 3C and 3D, the number of autophagosomes of miR-9-5p mimics group was less than NC group. After 4Gy doses of radiation, the number of autophagosomes of both groups were all increased. Moreover, we measured the expression of tubule form related protein and autophagy-related protein by Western blot. As shown in Figure 3E, upregulation of miR-9-5p accelerated p-VEGFR2, p-ERK, VEGFA, p62, p-ULK accumulation but impaired LC3-II accumulation. After 4Gy doses of radiation, the accumulation of p-VEGFR2, p-ERK, VEGFA were all decreased, but the autophagy-related protein was increased.

SOCS5 Was a Target Gene of MiR9-5p and Low Expression in Cervical Cancer

We used the bioinformatics database TargetScan and miRanda to predict the target genes of miR-9-5p and preliminarily screened the predicted genes. Through the NCBI gene search and literature retrieval, we finally selected SOCS5 as a potential target gene of miR-9-5p (Figure 4A). A dual-luciferase reporter assay was subsequently employed to verify the binding sites for miR-9-5p in the SOCS5 3'UTR region. Upregulation of miR-9-5p decreased the luciferase activity of cells transfected with wild-type SOCS5 vector (Figure 4B). Then, we used immunohistochemical staining to analyze the protein expression of SOCS5 in 30 cases of cervical cancer and adjacent normal tissues. The results showed that SOCS5 positive staining was mainly in the cytoplasm, with a low expression ratio of 83.3% and a high expression ratio of 16.7% in cervical cancer tissues, while the high expression ratio of 73.3% and the low expression ratio of 26.7% in adjacent normal tissues (Figure 4C and 4D).

Overexpression of SOCS5 Could Inhibit MiR-9-5p Mimics from Promoting Tubule Formation

MiR-9-5p could promote the formation of tubules and regulated the expression of SOCS5 (Figure 5A), which is a tumor suppressor gene. We transfected SiHa with SOCS5-LV and miR-9-5p mimics, the tubule-forming ability of HUVEC cells was then tested. As shown in Figure 5A and 5B, after transfected with miR-9-5p mimics, the numbers of tube formation were significantly decreased in the SOCS5 overexpression group than the control group. Western blot detected the corresponding changes in tubule-formation related molecules and EMT targets (Figure 5C).

MiR-9-5p Promoted Primary Tumor Growth In Vivo

Further, orthotopic xenograft mouse models were introduced to assess the effect of miR-9-5p on CC cell tumorigenesis *in vivo*. SiHa transfected with miR-9-5p mimics or miR-NC were inoculated into nude mice, and after 4 weeks, the mice were sacrificed, and the tumor volume was measured. As shown in Figure 6A and 6B, the tumors volume from mice in the miR-9-5p overexpression group was significantly larger compared with the control group. With the extension of time, the tumors volume gradually increased, and the volume of miR-9-5p mimics group was significantly larger than that of miR-NC group (Figure 6C). The results indicated that miR-9-5p may promote the proliferation of cervical cancer *in vivo*.

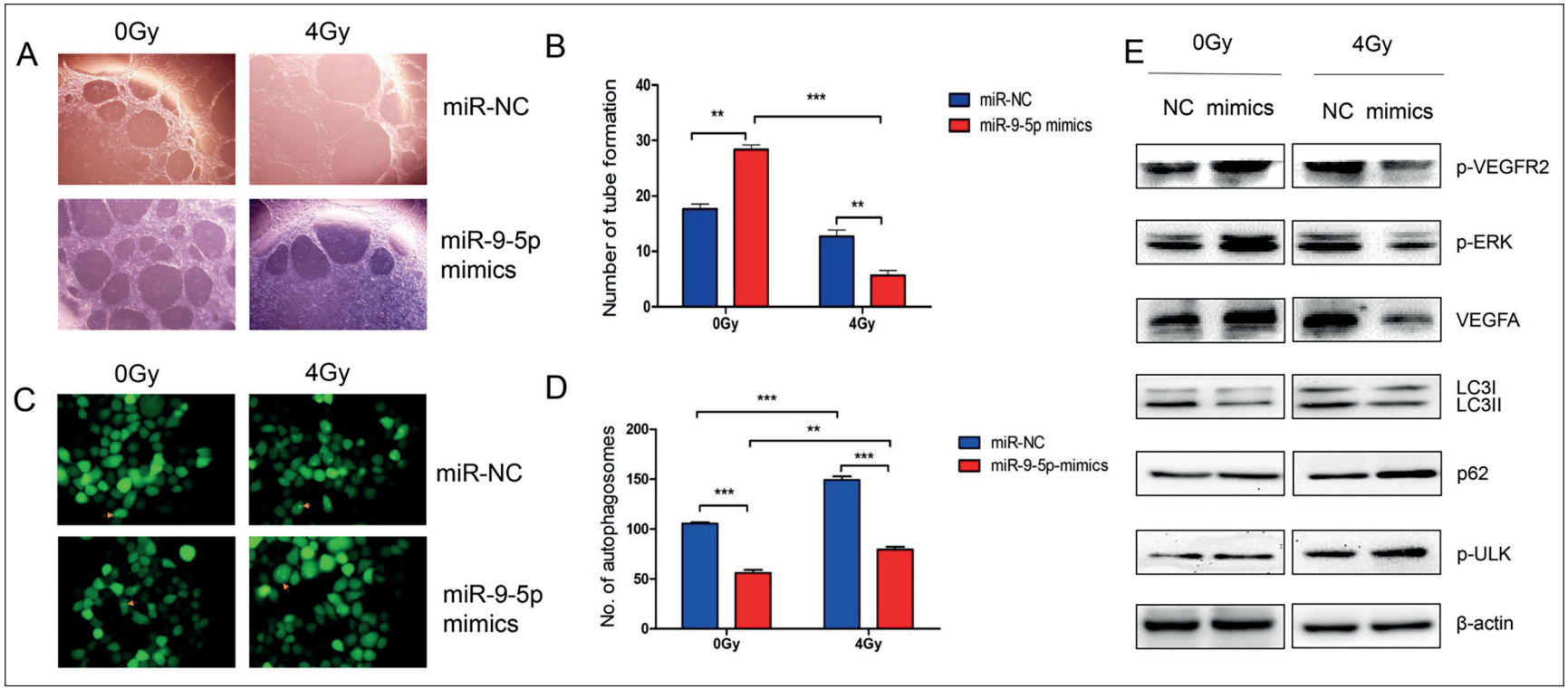

Figure 3. MiR-9-5p affected the radiosensitivity of cervical cancer cells to γ radiation. ***A, B,*** Effects of miR-9-5p on tubule formation under 4 doses of γ radiation (magnification: 2,000×). The results are expressed as the mean±standard deviation. **p<0.01, ***p<0.001. ***C, D,*** Autophagomsomes (green channel) in SiHa transfected with miR-NC or miR-9-5p mimics after 4Gy γ radiation. The results are expressed as the mean±standard deviation (magnification: 200×). **p<0.01, ***p<0.001. ***E,*** Autophagy related markers (p62, p-ULK and LC3), p-VEGFR2, p-ERK, VEGFA were tested by Western blot when transfected cells with or without irradiation.

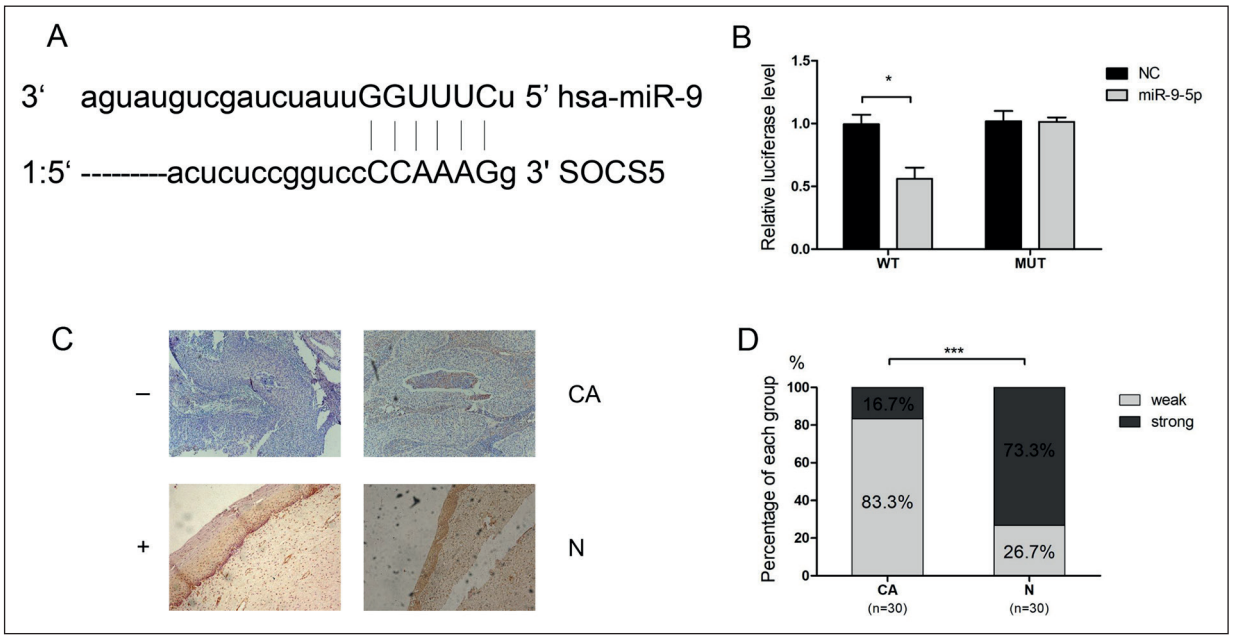

Figure 4. SOCS5, target gene of miR9-5p, low expression in cervical cancer. ***A,*** TargetScan and miRanda predicted the potential site of the 3`UTR region of SOCS5 mRNA binding to miR-9-5p. ***B,*** Reporter vectors with wild-type or mutant SOCS5 3'UTRs were co-transfected with miR-9-5p mimics in SiHa and the relative luciferase activities are shown. ***C,*** Representative images of immunohistochemical staining of SOCS5 in the cancer tissues and normal cervical tissues (magnification: 100×). ***D,*** Distribution of immunohistochemical score, showed in histogram, indicates that SOCS5 is weak expression in CC. ***$p<0.001$.

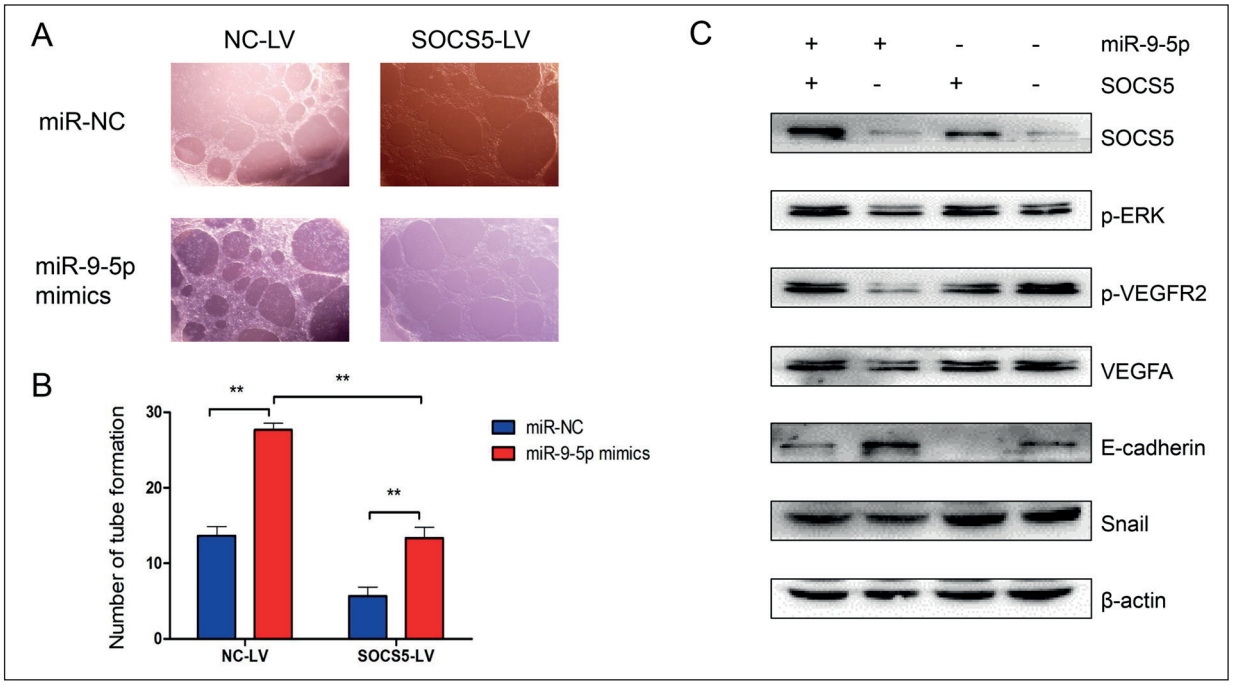

Figure 5. Overexpression of SOCS5 could inhibit miR-9-5p mimics from promoting tubule formation. ***A, B,*** After transfected with miR-9-5p mimics, the numbers of tube formation was significantly decreased in the SOCS5 overexpression group than the control group (magnification: 2,000×). ***C,*** Western blot detected tubule-formation related molecules and EMT targets. SiHa transfected with SOCS5-LV and miR-9-5p mimics. NC-LV: pHBLV-CMV-MCS-3flag-Zsgreen-puro negative control; SOCS5-LV: pHBLV-CMV-MCS-3flag-Zsgreen-puro tagged SOCS5.

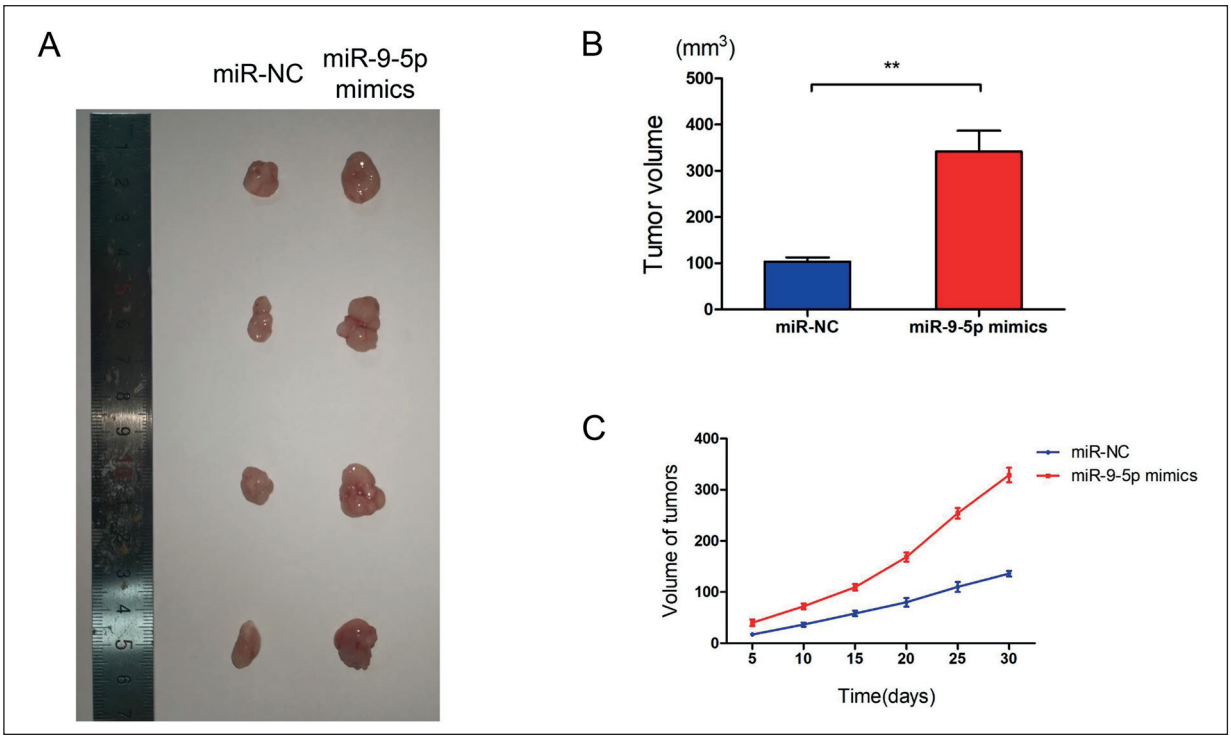

Figure 6. MiR-9-5p accelerated tumor growth *in vivo*. ***A,*** SiHa cells with or without miR-9-5p overexpression were subcutaneously inoculated into nude mice. Each group contains 4 mice. ***B,*** Tumor volumes of control and miR-9-5p mimics. ***C,*** Growth curves of tumors` volume in control and miR-9-5p overexpression group.

Discussion

Cervical cancer is a common gynecological malignancy and is one of the leading causes of cancer-related mortality in women worldwide[15,16]. Radiotherapy, chemotherapy, and surgery are standard treatments for cervical cancer, but the 5-year survival rate of patients with advanced disease is still very low[17,18]. Lymph nodes and distant organ metastasis have been reported to be the main cause of treatment failure[19,20]. At present, the molecular mechanism that reveals the development of cervical cancer is of great significance for individualized treatment. More and more miRNA have been shown to be involved in the development and progression of various human malignancies and may become new diagnostic and prognostic markers[21-23]. MiR-487a, mediated by heat shock factor 1, promotes proliferation and metastasis of hepatocellular carcinoma[24]. Ectopic expression of miR-3978 in the MKN45 cell line significantly reduced cell proliferation and inhibited cell migration, and invasion, and the miR-3978 mimic inhibited the progression of metastasis in gastric cancer mice models by regulating the expression of legumain protein[25]. MiR-9-5p promoted the proliferation, metastasis and invasion of non-small cell lung cancer (NSCLC) cells[26] and we found similar phenomena in cervical cancer cells. It has been reported that miR-9 mediated down-regulation of E-cadherin leads to activation of β-catenin signaling, resulting in upregulation of genes encoding vascular endothelial growth factor (VEGF) and in turn leads to increased tumor angiogenesis[27]. In our research, we first found that miR-9-5p expression was significantly higher in patients with positive lymph nodes of cervical cancer than in patients with negative lymph nodes. We also observed that miR-9-5p promotes the proliferation and invasion of cervical cancer cells. MiR-9-5p may sensitize tumor cells to EMT-inducing signals arising from the tumor microenvironment. This results in cancer cells gaining interstitial features later in tumor progression, which in turn may contribute to metastatic spread.

In addition, recent evidence suggests that a variety of miRNAs are involved in therapeutic response and play an important role in radiation. For instance, miR-208a could affect the

radiosensitivity of human lung cancer cells by targeting p21[28]. Overexpression of MiR-200c increases the radiosensitivity of breast cancer cells by inhibiting cell proliferation, increasing apoptosis, and DNA double-strand breaks[29]. A high expression of miR-9 also significantly enhanced the radiosensitivity of NSCLC[30]. Overexpression of miR-145 enhanced radiosensitivity of cervical cancer by inhibiting cell viability and increasing radiation-induced apoptosis[31]. Recently, targeting the tumor vasculature to "starve a tumor to death" has become a clinical cancer therapy strategy along with chemotherapy and radiotherapy[32]. VEGF is one of the most critical pro-angiogenic factors which mediated through VEGF receptor 2 (VEGFR2)[33]. In the current study, we discovered that miR-9-5p as a positive regulator of angiogenesis *via* targeting VEGFR2. Moreover, after the radiation dose of 4Gy, tubule generation in miR-9-5p mimics group was significantly reduced compared with that in control group. MiR-9-5p contributes to enhancing the radiosensitivity of cervical cancer cells.

Many cellular processes, such as DNA damage repair, cell cycle arrest, and autophagy, are involved in the development of radio-resistance[34]. Accumulating evidence[35,36] indicates that the autophagic response of cancer cells to radiation may have a major role in cellular survival. It has been reported that miRNAs can regulate the levels of autophagy in cells, while autophagy levels can, in turn, regulate the expression of miRNAs[37]. In our results, the overexpression of miR-9-5p causes a change in autophagy, which was consistent with the protein expression results after given the radiation. Results encouraged us further examining the mechanism of cervical cancer radioresistance related to miR-9-5p and its effects on cellular pathways leading to cervical cancer progression.

We indicated that SOCS5, as a target of miR-9-5p, is a tumor suppressor in cervical cancer. Several studies[38-40] have found that SOCS5 may be regulated by miRNAs, such as miR-302a-3p, miR-885-5p, miR-18/miR-25 and so on. Our analysis showed that miR-9-5p targets SOCS5 and SOCS5 expression was shown to be downregulated when miR-9-5p was overexpressed, resulting in increased EMT transition and tube formation.

This is the first report showing miR-9-5p as a potential oncomiR in cervical cancer that promotes tumor growth, invasion, and angiogenesis by targeting SOCS5. MiR-9-5p regulated autophagy and contributed to a radiosensitizing effect.

Conclusions

MiR-9-5p may be a novel radiosensitizing target in cervical cancer. This opens up new opportunities for further research into alternative approaches to cervical cancer treatment targets.

Conflict of Interest

The Authors declare that they have no conflict of interests.

References

1) Bray F, Ferlay J, Soerjomataram I, Siegel RL, Torre LA, Jemal A. Global cancer statistics 2018: GLOBOCAN estimates of incidence and mortality worldwide for 36 cancers in 185 countries. CA Cancer J Clin 2018; 68: 394-424.
2) Wang J, Bai Z, Wang Z, Yu C. Comparison of secular trends in cervical cancer mortality in China and the United States: an age-period-cohort analysis. Int J Environ Res Public Health 2016; 13. pii: E1148.
3) Wieringa HW, van der Zee AG, de Vries EG, van Vugt MA. Breaking the DNA damage response to improve cervical cancer treatment. Cancer Treat Rev 2016; 42: 30-40.
4) Wang W, Chu HJ, Shang CL, Gong X, Liu TY, Zhao YH, Huang JM, Yao SZ. Long-term oncological outcomes after laparoscopic vs. abdominal radical hysterectomy in stage IA2 to IIA2 cervical cancer: a matched cohort study. Int J Gynecol Cancer 2016; 26: 1264-1273.
5) Mirnezami AH, Pickard K, Zhang L, Primrose JN, Packham G. MicroRNAs: key players in carcinogenesis and novel therapeutic targets. Eur J Surg Oncol 2009; 35: 339-347.
6) Finoux AL, Chartrand P. [Oncogenic and tumour suppressor microRNAs]. Med Sci (Paris) 2008; 24: 1049-1054.
7) Bartel DP. MicroRNAs: target recognition and regulatory functions. Cell 2009; 136: 215-233.
8) Osaki M, Takeshita F, Ochiya T. MicroRNAs as biomarkers and therapeutic drugs in human cancer. Biomarkers 2008; 13: 658-670.
9) Laios A, O'Toole S, Flavin R, Martin C, Kelly L, Ring M, Finn SP, Barrett C, Loda M, Gleeson N, D'Arcy T, McGuinness E, Sheils O, Sheppard B, O' Leary J. Potential role of miR-9 and miR-223 in recurrent ovarian cancer. Mol Cancer 2008; 7: 35.
10) Rotkrua P, Akiyama Y, Hashimoto Y, Otsubo T, Yuasa Y. MiR-9 downregulates CDX2 expression in gastric cancer cells. Int J Cancer 2011; 129: 2611-2620.
11) Xiao Y, Zhang Y, Chen Y, Li J, Zhang Z, Sun Y, Shen H, Zhao Z, Huang Z, Zhang W, Chen W, Shen Z.

Inhibition of microRNA-9-5p protects against cardiac remodeling following myocardial infarction in mice. Hum Gene Ther 2019; 30: 286-301.

12) Li X, He L, Yue Q, Lu J, Kang N, Xu X, Wang H, Zhang H. MiR-9-5p promotes MSC migration by activating beta-catenin signaling pathway. Am J Physiol Cell Physiol 2017; 313: C80-C93.

13) Yi J, Gao ZF. MicroRNA-9-5p promotes angiogenesis but inhibits apoptosis and inflammation of high glucose-induced injury in human umbilical vascular endothelial cells by targeting CXCR4. Int J Biol Macromol 2019; 130: 1-9.

14) Vojtechova Z, Sabol I, Salakova M, Smahelova J, Zavadil J, Turek L, Grega M, Klozar J, Prochazka B, Tachezy R. Comparison of the miRNA profiles in HPV-positive and HPV-negative tonsillar tumors and a model system of human keratinocyte clones. BMC Cancer 2016; 16: 382.

15) Yuan Y, Min SJ, Xu DQ, Shen Y, Yan HY, Wang Y, Wang W, Tan YJ. Expressions of VEGF and miR-21 in tumor tissues of cervical cancer patients with HPV infection and their relationships with prognosis. Eur Rev Med Pharmacol Sci 2018; 22: 6274-6279.

16) Ferlay J, Shin HR, Bray F, Forman D, Mathers C, Parkin DM. Estimates of worldwide burden of cancer in 2008: GLOBOCAN 2008. Int J Cancer 2010; 127: 2893-2917.

17) Derks M, Biewenga P, van der Velden J, Kenter GG, Stalpers LJ, Buist MR. Results of radical surgery in women with stage IB2/IIA2 cervical cancer. Acta Obstet Gynecol Scand 2016; 95: 166-172.

18) Meijer CJ, Snijders PJ. Cervical cancer in 2013: screening comes of age and treatment progress continues. Nat Rev Clin Oncol 2014; 11: 77-78.

19) Vandeperre A, Van Limbergen E, Leunen K, Moerman P, Amant F, Vergote I. Para-aortic lymph node metastases in locally advanced cervical cancer: comparison between surgical staging and imaging. Gynecol Oncol 2015; 138: 299-303.

20) Cohen PA, Jhingran A, Oaknin A, Denny L. Cervical cancer. Lancet 2019; 393: 169-182.

21) Farazi TA, Spitzer JI, Morozov P, Tuschl T. MiRNAs in human cancer. J Pathol 2011; 223: 102-115.

22) Calin GA, Ferracin M, Cimmino A, Di Leva G, Shimizu M, Wojcik SE, Iorio MV, Visone R, Sever NI, Fabbri M, Iuliano R, Palumbo T, Pichiorri F, Roldo C, Garzon R, Sevignani C, Rassenti L, Alder H, Volinia S, Liu CG, Kipps TJ, Negrini M, Croce CM. A microRNA signature associated with prognosis and progression in chronic lymphocytic leukemia. N Engl J Med 2005; 353: 1793-1801.

23) Chen X, Ba Y, Ma L, Cai X, Yin Y, Wang K, Guo J, Zhang Y, Chen J, Guo X, Li Q, Li X, Wang W, Zhang Y, Wang J, Jiang X, Xiang Y, Xu C, Zheng P, Zhang J, Li R, Zhang H, Shang X, Gong T, Ning G, Wang J, Zen K, Zhang J, Zhang CY. Characterization of microRNAs in serum: a novel class of biomarkers for diagnosis of cancer and other diseases. Cell Res 2008; 18: 997-1006.

24) Chang RM, Xiao S, Lei X, Yang H, Fang F, Yang LY. MiRNA-487a promotes proliferation and metastasis in hepatocellular carcinoma. Clin Cancer Res 2017; 23: 2593-2604.

25) Zhang Y, Wu YY, Jiang JN, Liu XS, Ji FJ, Fang XD. MiRNA-3978 regulates peritoneal gastric cancer metastasis by targeting legumain. Oncotarget 2016; 7: 83223-83230.

26) Li G, Wu F, Yang H, Deng X, Yuan Y. MiR-9-5p promotes cell growth and metastasis in non-small cell lung cancer through the repression of TGFBR2. Biomed Pharmacother 2017; 96: 1170-1178.

27) Ma L, Young J, Prabhala H, Pan E, Mestdagh P, Muth D, Teruya-Feldstein J, Reinhardt F, Onder TT, Valastyan S, Westermann F, Speleman F, Vandesompele J, Weinberg RA. MiR-9, a MYC/MYCN-activated microRNA, regulates E-cadherin and cancer metastasis. Nat Cell Biol 2010; 12: 247-256.

28) Tang Y, Cui Y, Li Z, Jiao Z, Zhang Y, He Y, Chen G, Zhou Q, Wang W, Zhou X, Luo J, Zhang S. Radiation-induced miR-208a increases the proliferation and radioresistance by targeting p21 in human lung cancer cells. J Exp Clin Cancer Res 2016; 35: 20.

29) Lin J, Liu C, Gao F, Mitchel RE, Zhao L, Yang Y, Lei J, Cai J. MiR-200c enhances radiosensitivity of human breast cancer cells. J Cell Biochem 2013; 114: 606-615.

30) Xiong K, Shao LH, Zhang HQ, Jin L, Wei W, Dong Z, Zhu YQ, Wu N, Jin SZ, Xue LX. MicroRNA-9 functions as a tumor suppressor and enhances radio-sensitivity in radio-resistant A549 cells by targeting neuropilin 1. Oncol Lett 2018; 15: 2863-2870.

31) Ye C, Sun NX, Ma Y, Zhao Q, Zhang Q, Xu C, Wang SB, Sun SH, Wang F, Li W. MicroRNA-145 contributes to enhancing radiosensitivity of cervical cancer cells. FEBS Lett 2015; 589: 702-709.

32) Ichihara E, Kiura K, Tanimoto M. Targeting angiogenesis in cancer therapy. Acta Med Okayama 2011; 65: 353-362.

33) Olsson AK, Dimberg A, Kreuger J, Claesson-Welsh L. VEGF receptor signalling - in control of vascular function. Nat Rev Mol Cell Biol 2006; 7: 359-371.

34) Ahmed KM, Li JJ. ATM-NF-kappaB connection as a target for tumor radiosensitization. Curr Cancer Drug Targets 2007; 7: 335-342.

35) Zois CE, Koukourakis MI. Radiation-induced autophagy in normal and cancer cells: towards novel cytoprotection and radio-sensitization policies? Autophagy 2009; 5: 442-450.

36) Chaachouay H, Ohneseit P, Toulany M, Kehlbach R, Multhoff G, Rodemann HP. Autophagy contributes to resistance of tumor cells to ionizing radiation. Radiother Oncol 2011; 99: 287-292.

37) Jing Z, Han W, Sui X, Xie J, Pan H. Interaction of autophagy with microRNAs and their potential therapeutic implications in human cancers. Cancer Lett 2015; 356: 332-338.

38) Zhang Z, Li J, Guo H, Wang F, Ma L, Du C, Wang Y, Wang Q, Kornmann M, Tian X, Yang Y. BRM transcriptionally regulates miR-302a-3p to target SOCS5/STAT3 signaling axis to potentiate pancreatic cancer metastasis. Cancer Lett 2019; 449: 215-225.

39) Su M, Qin B, Liu F, Chen Y, Zhang R. MiR-885-5p upregulation promotes colorectal cancer cell proliferation and migration by targeting suppressor of cytokine signaling. Oncol Lett 2018; 16: 65-72.

40) Sanchez-Mejias A, Kwon J, Chew XH, Siemens A, Sohn HS, Jing G, Zhang B, Yang H, Tay Y. A novel SOCS5/miR-18/miR-25 axis promotes tumorigenesis in liver cancer. Int J Cancer 2019; 144: 311-321.